

Efficient channel waveguide lasers in monoclinic double tungstates: towards further integration with on-chip mirrors

K. van Dalfsen,¹ H. A. G. M. van Wolferen,² M. Dijkstra,¹ S. Aravazhi,¹
E. H. Bernhardt,¹ S. M. García-Blanco,¹ and M. Pollnau¹

¹ Integrated Optical Microsystems Group

² Transducers Science and Technology Group

MESA+ Institute for Nanotechnology, University of Twente, Enschede

By varying the thulium concentration in the range of 1.5 – 8.0 at.% in thulium-gadolinium-lutetium-yttrium-co-doped monoclinic double tungstate channel waveguides, a maximum laser slope efficiency of 70% with respect to the absorbed pump power was obtained. Further integration of these channel waveguides with on-chip mirrors will combine high slope efficiencies and output powers with narrow-line spectral laser characteristics. A silicon nitride layer was deposited onto a planar thulium-co-doped monoclinic double tungstate layer, and subsequently covered by a metal mask. Strip-loaded, corrugated channel waveguides defined by electron-beam lithography were etched into the silicon nitride layer by means of reactive ion etching.

Introduction

The fabrication of lasers in monoclinic double tungstates has advanced from bulk and planar waveguide lasers toward the recent demonstration of channel waveguide lasers in the 1- μm and 2- μm wavelength regions [1-3]. Not only do these lasers provide a footprint reduction and low thresholds, but also appreciable output powers of several hundreds of milliWatts and slope efficiencies to a maximum of 71% in case of Yb^{3+} -doped monoclinic double tungstates. A drawback to these lasers is that the mirrors are not integrated, requiring the rather unstable butt-coupling of mirrors. Further integration of the lasers with on-chip mirrors [4] is naturally the next step towards integrated channel waveguide lasers in this material. In this paper, we present a method for the fabrication of corrugated, strip-loaded channel waveguides based on silicon nitride (SiN) on monoclinic double tungstates, by using electron-beam technology to define the corrugated channels in a one-step lithographic process [5].

Fabrication

Yttrium-gadolinium-lutetium-thulium-co-doped layers were grown by liquid-phase epitaxy at 920–923°C in a $\text{K}_2\text{W}_2\text{O}_7$ solvent, onto pure $\text{KY}(\text{WO}_4)_2$ (=KYW) substrates. Compared to the pure KYW substrate, where the amount of Y^{3+} per crystal unit cell is 100%, the overgrown layer has lower amounts of Y^{3+} , compensated by co-doping with Gd^{3+} , Lu^{3+} and Tm^{3+} , with $\text{Y}^{3+} + \text{Gd}^{3+} + \text{Lu}^{3+} + \text{Tm}^{3+} = 100\%$. The refractive index contrast of the grown layers with the pure KYW substrates is determined predominantly by the amount of Lu^{3+} in the layer. The addition of Gd^{3+} is required to minimize the lattice stress of the overgrown layer with the pure KYW substrate, as the larger ionic radius of the Gd^{3+} compensates the smaller ionic radius of Lu^{3+} . Different compositions with index contrasts of 1×10^{-2} (buried channels) and 2×10^{-2} (ridge-type channels with air cladding) with the pure KYW substrate (at 1550 nm and transverse-magnetic

polarization, $E||N_p$), and with thulium doping levels of 1.5–8at.% were obtained. The layers with an index contrast of 1×10^{-2} were lapped and surface-polished to a laser-grade quality with a planar layer thickness of 7.7 μm and 14.3 μm , covered with a photoresist mask, and patterned 1.9 μm deep by Ar^+ -beam milling. The resulting ridge channel waveguides had a width of 10-25 μm , and were overgrown with a pure KYW cladding layer. These samples were diced and end-face polished to a length of 6.7 mm and 4.2 mm, respectively.

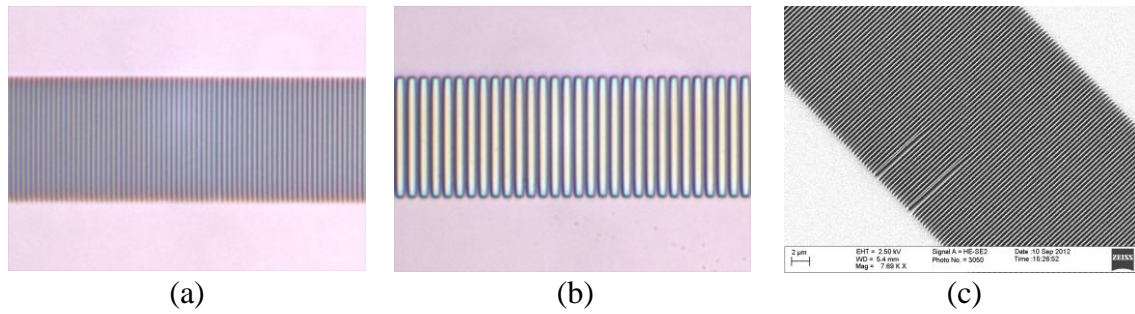


Fig 1. Strip-loaded, corrugated silicon nitride channel waveguide structures on a co-doped, planar monoclinic double tungstate layer with a period of a) $\sim 0.5 \mu\text{m}$, b) $1.18 \mu\text{m}$. c) Scanning electron microscope image of a corrugated channel with a period of $\sim 500 \text{ nm}$.

The layers with an index contrast of 2×10^{-2} with the substrate were lapped and polished to a laser-grade quality with a planar layer thickness of $\sim 3 \mu\text{m}$, and a silicon nitride (SiN) layer with a thickness of $\sim 400 \text{ nm}$ was deposited onto the thulium-co-doped planar layer by PECVD. A 45-nm-thick chromium mask was subsequently sputtered onto the SiN layer, followed by the deposition of an electron-beam-compatible resist with a thickness of $\sim 180 \text{ nm}$. Uncorrugated channels and two types of corrugated channel waveguide patterns, the first type with a width of 20 μm , and a periodicity of $\sim 500 \text{ nm}$ and a duty cycle of 50% and the second type with a period of 1.18 μm and a duty cycle of 65%, were written into the e-beam resist using a Raith 150^{TWO} e-beam lithographic system. The channels are aligned such that the light propagates along the N_g optical axis. The pattern was developed and etched into the chromium layer by wet etching. Finally, the pattern was transferred into the SiN layer by etching 400-nm deep using reactive ion etching. Finally, the chromium mask residue was removed, and the gratings covered with a 9/135 standard photoresist acting as a protective layer. The sample was diced and end-face polished to a length of $\sim 6 \text{ mm}$, after which the photoresist layer was removed.

Experimental setup

Laser experiments on 1.5at.%, 5.0 at.% and 8.0at.% Tm^{3+} -doped samples were performed by butt-coupling of dielectric mirrors R_1 and R_2 to the channel front and back end-facets, respectively, to obtain a reflectivity of $R_1 = 99.9\%$ and $R_2 = 98\%$, $R_1 = 99.9\%$ and $R_2 = 92\%$, $R_1=99.9\%$ and $R_2 = 11\%$, and $R_1 = R_2 = 11\%$. A reflectivity of $R_1, R_2 = 11\%$ refers to the Fresnel reflection in case no butt-coupled mirror was placed. Pump power at 794 nm in TM polarization ($E||N_p$) and 802 nm in TE polarization ($E||N_m$) from a Ti:Sapphire laser was coupled into the channel waveguides by using two cylindrical lenses with focal lengths of 40 mm and 10 mm in horizontal and vertical direction, respectively. The laser output power was out-coupled from the other waveguide end via a microscope objective with a numerical aperture of $\text{NA} = 0.25$ and

measured. The laser light was passed through a RG1000 high-pass filter to block any residual pump power. The laser wavelength was measured using a spectrometer.

The transmission of the grating with a period of $1.18 \mu\text{m}$, which acts as a third-order grating at 1550 nm , was characterized with a tuneable laser around between 1460 nm and 1620 nm , for TE and TM polarization. To this end, a polarization-maintaining (PM) fiber was connected to the tuneable laser and butt-coupled to the channel end-facet. A standard $9 \mu\text{m}$ fiber was butt-coupled to the other end-facet of the channel and fed to a photo detector.

Laser results and grating transmission

The measured laser output power versus absorbed pump power when pumping the 8.0at. %-doped sample at 794 nm in TM polarization or 802 nm in TE polarization is shown in Figs. 1(a) and 1(b), respectively. The maximum output power obtained is 300 mW for both TE and TM polarizations. A maximum slope efficiency of 70% with respect to the absorbed pump power is obtained with 99% out-coupling while pumping in TM polarization [6]. The slope efficiencies and output powers are comparable up to a few percent for both pump polarizations, as would be expected from basic laser theory.

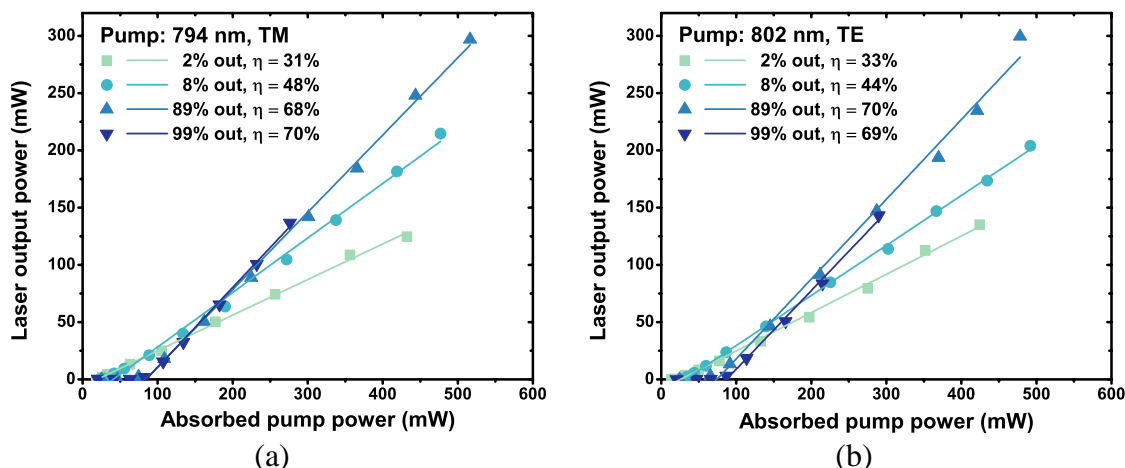


Fig 2. a) Output power versus absorbed pump power of an 8 at. % thulium-doped channel waveguide laser pumped at (a) 794 nm in TM polarization and (b) 802 nm in TE polarization. Taken from [6].

The transmission spectra of a strip-loaded, corrugated SiN waveguide on a monoclinic double tungstate planar waveguide, measured for TM and TE polarizations are shown in Figs 3(a) and 3(b), respectively. This particular grating exhibits a third-order periodicity at 1550 nm due to the combination of the effective refractive index of the optical mode at 1550 nm ($N_{\text{eff}} = 1.960$ for TM, $N_{\text{eff}} = 1.994$ for TE) and the grating period of $1.18 \mu\text{m}$. The transmission dip for TM polarization is located at 1549 nm , whereas the transmission dip for TE polarization is located at 1574 nm . This difference of $\sim 25 \text{ nm}$ corresponds to the difference of the effective refractive indices for the two polarizations. The depth of the transmission dips is approximately 0.5 dB . It is however difficult to extract the reflectivity from this, as radiation into the air cladding and into the pure KYW substrate contributes strongly to the losses, due to the third order nature of the grating at this wavelength. The results can hence only be interpreted as a confirmation that the gratings do have an effect on the optical mode, and most important, that the Bragg wavelength found in this measurement corresponds to the expected Bragg wavelength. The highly oscillatory nature of the graphs is caused by the Fresnel

reflections of the end-facets. Using index-matching fluid between the fibers and end-facets will alleviate this effect.

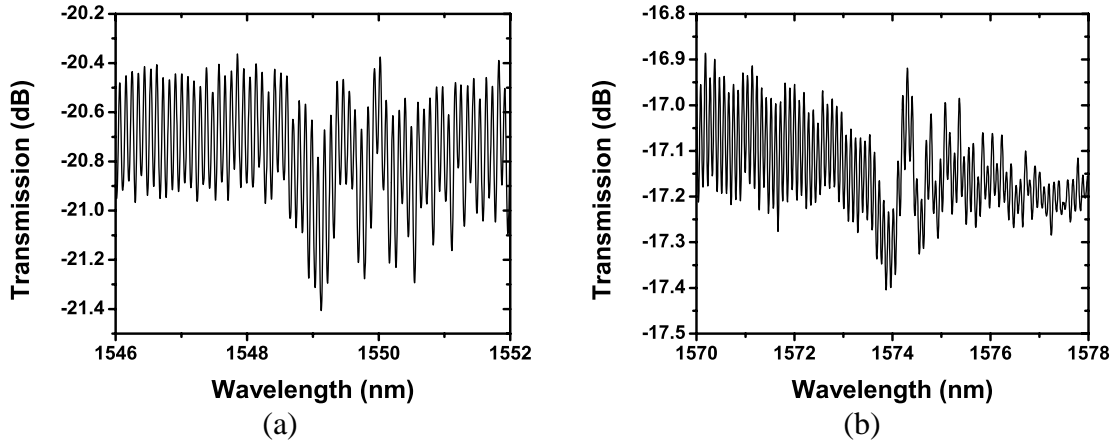


Fig 3. Measured transmission spectra for TM (a) and TE (b) polarization of a corrugated, strip-loaded channel waveguide in SiN on top of a monoclinic double tungstate planar waveguide.

Conclusions

Highly efficient channel waveguide lasers based on thulium-doped monoclinic double tungstates have been demonstrated with a maximum slope efficiency of 70%, and output powers up to 300 mW. Planar waveguide layers of this highly efficient material are being combined with strip-loaded, corrugated SiN channel waveguides to obtain on-chip mirrors for the realization of distributed-feedback (DFB) or distributed Bragg reflector (DBR) lasers. To this end, patterning of these corrugated, strip-loaded channel waveguides via electron-beam lithography has been demonstrated, and preliminary results of a third-order grating at 1550 nm show a dip in the transmission spectrum at wavelengths corresponding to the Bragg frequency of the designed waveguides. Further characterization of the first- and third-order gratings to determine the reflectivity is ongoing, and lasing experiments exploiting the reflectivity of the first-order gratings.

References

- [1] D. Geskus, S. Aravazhi, K. Wörhoff, and M. Pollnau, "High-power, broadly tunable, and low-quantum-defect $\text{KGd}_{1-x}\text{Lu}_x(\text{WO}_4)_2:\text{Yb}^{3+}$ channel waveguide lasers," *Opt. Express* 18, 26107–26112 (2010).
- [2] W. Bolaños, J. J. Carvajal, X. Mateos, G. S. Murugan, A. Z. Subramanian, J. S. Wilkinson, E. Cantelar, D. Jaque, G. Lifante, M. Aguiló, and F. Díaz, "Mirrorless buried waveguide laser in monoclinic double tungstates fabricated by a novel combination of ion milling and liquid phase epitaxy," *Opt. Express* 18, 26937–26945 (2010).
- [3] K. van Daltsen, S. Aravazhi, D. Geskus, K. Wörhoff, and M. Pollnau, "Efficient $\text{KY}_{1-x}\text{Gd}_x\text{Lu}_y(\text{WO}_4)_2:\text{Tm}^{3+}$ channel waveguide lasers," *Opt. Express* 19, 5277–5282 (2011).
- [4] E. H. Bernhardt, H. A. G. M. van Wolferen, L. Agazzi, M. R. H. Khan, C. G. H. Roeloffzen, K. Wörhoff, M. Pollnau, and R. M. de Ridder, "Ultra-narrow-linewidth, single-frequency distributed feedback waveguide laser in $\text{Al}_2\text{O}_3:\text{Er}^{3+}$ on silicon," *Opt. Lett.* 35, 2394–2396 (2010).
- [5] M. A. Mohammad, T. Fito, J. Chen, S. Buswell, M. Aktary, M. Stepanova, and S. K. Dew, "Systematic study of the interdependence of exposure and development conditions and kinetic modelling for optimizing low-energy electron beam nanolithography," *Microelectron. Eng.* 87, 1104–1107 (2010).
- [6] K. van Daltsen, S. Aravazhi, C. Grivas, S. M. García-Blanco, and M. Pollnau, "Thulium channel waveguide laser in a monoclinic double tungstate with 70% slope efficiency," *Opt. Lett.* 37, 887–889 (2012).